Modelling the Mechanical Properties of Hydroxyapatite Scaffolds Produced by Digital Light Processing-Based Vat Photopolymerization †

Francesco Baino [1,*] , **Martin Schwentenwein** [2] **and Enrica Verné** [1]

1   Institute of Materials Physics and Engineering, Department of Applied Science and Technology (DISAT), Politecnico di Torino, 10129 Torino, Italy
2   Lithoz GmbH, 1060 Vienna, Austria
*   Correspondence: francesco.baino@polito.it
†   Dedicated to the cherished memory of Giovanni Argiolas.

Abstract: Porosity is a key feature in dictating the overall performance of biomedical scaffolds, with special relevance to mechanical properties. Usually, compressive strength and elastic modulus are the main parameters used to determine the potential mechanical suitability of porous scaffolds for bone repair. However, their assessment may not be so easy from an experimental viewpoint and, especially if the porosity is high, so reliable for brittle bioceramic foams. Hence, assessing the relationship between porosity and mechanical properties based only on the constitutive parameters of the solid material is a challenging and important task to predict the scaffold performance for optimization during design. In this work, a set of equations was used to predict the compressive strength and elastic modulus of bone-like hydroxyapatite scaffolds produced by digital light processing-based vat photopolymerization (total porosity about 80 vol.%). The compressive strength was found to depend on total porosity, following a power-law approximation. The relationship between porosity and elastic modulus was well fitted by second-order power law, with relative density and computational models obtained by numerical simulations.

Keywords: hydroxyapatite; scaffold; additive manufacturing; elastic modulus; compressive strength; bone repair

1. Introduction

Implantable biomaterials are often designed as porous scaffolds that serve as three-dimensional (3D) templates to support and guide the healing of osseous tissue at the injured site [1]. Hydroxyapatite is one of the most popular biomaterials for bone substitution due to its similarity with the calcium-phosphate mineral phase of natural bone [2]. Hydroxyapatite has been clinically used for decades in multiple forms, including micro-sized and nano-sized particles, coatings on metallic endoprostheses, composites, injectable pastes for spine surgery and porous scaffolds [3]. Conventional methods to fabricate porous hydroxyapatite products rely on foaming methods or on the mixing of the ceramic powders with pore-forming agents, such as polymeric grains or an organic porous template, followed by high-temperature treatments to burn-off the sacrificial substances and sinter the inorganic particles [4]. As a result, a porous product is obtained, in which the pore characteristics and architecture, e.g., total pore volume, pore size, pore interconnectivity, depend on multiple factors, including distribution of hydroxyapatite particle size, type of fabrication method used, type of pore-forming agent/template used, and sintering conditions [5].

The application of computer aided design (CAD) and computer aided manufacturing (CAM) technologies to biomaterials allowed improvements in the control of pore geometry and architecture, as well as the repeatability and scalability of the production process, thus opening new horizons in the field of porous hydroxyapatite and ceramic scaffolds. A

review paper on the potential and challenges of additive manufacturing of hydroxyapatite and hydroxyapatite-based composite scaffolds has been recently published [6].

At present, the best spatial resolution (less than 50 μm) and, hence, the highest quality of ceramic products can be obtained by vat photopolymerization, also known as stereolithography. The latest evolution of this method relies on digital light processing (DLP), involving the use of a dynamic mask to promote the single-step polymerization of a photocurable resin layer with embedded ceramic particles. Compared to other additive manufacturing technologies, this bottom-up method is faster, yields fewer defects in the printed product, and less material is required during the printing process [7].

Despite undeniable advantages, ceramic scaffolds produced by additive manufacturing technologies suffer from a typical grid-like arrangement of macro-channels and filaments, which reflects the structure of the CAD model used as the input file to the printing system [8]; thus, this simple porous architecture does not closely replicate the trabecular structure of cancellous bone.

On the contrary, sponge replication yields truly bone-like ceramic structures [9]. In order to overcome the limitation of grid-like channels, hydroxyapatite scaffolds were recently fabricated by this technology using a micro-tomographic reconstruction of an open-cell polyurethane foam as a CAD model input into the CAM system [10]. As a result, hydroxyapatite scaffolds with truly bone-like architecture, pore size and permeability were obtained.

An ideal scaffold for bone repair should fulfil a complex set of physico-chemical, mechanical and biological properties, including biocompatibility/bioactivity, architectural similarity to cancellous bone, and mechanical properties comparable to those of osseous tissue [11]. An overall porosity of at least 50 vol.% and a pore size in the range of 100–500 μm are recommended in bone tissue engineering applications to allow bio-fluid perfusion, cell colonization, and vasculature growth [12,13]. Microstructure and porosity also play a key role in dictating the mechanical properties of the scaffold, such as compressive strength and porosity. The former is relatively easy to assess, while the latter may be much more difficult to experimentally determine in highly porous ceramics. Knowledge of the elastic modulus is very important because a good match of stiffness between scaffold and bone allows favourable stress transfer, thereby yielding stable interfacial bonding and osteointegration [14].

Quantifying the relationship between the internal structure/porosity and mechanical properties of biomaterials still remains a partially unmet challenge. In this regard, the highly ambitious goal is the development and application of a general theory using the material's microstructural information (e.g., the constitutive properties of solid struts). In order to expand the knowledge in this field, a set of physical or numerical models were applied to describe the relationship between porosity and compressive strength/elastic modulus of hydroxyapatite scaffolds produced by DLP-based vat photopolymerization. To the best of our knowledge, this is the first time that such a study is performed on additively manufactured bioceramic scaffolds.

2. Materials and Methods

2.1. Fabrication and Characterization of Hydroxyapatite Scaffolds

The mechanical models for compressive strength and elastic modulus described in Section 2.2 were applied, for the first time, to foam-like hydroxyapatite scaffolds produced by DLP-based vat photopolymerization. The details of the scaffold fabrication process were reported in a previous study [10].

Briefly, the implemented manufacturing technique used the tomographic reconstruction of a polyurethane sponge as the input CAD file to the printing system. A multistep thermal treatment including sintering at 1300 °C for 2 h was then applied to printed "green" samples in order to remove organic binders and consolidate the ceramic scaffold.

The total porosity of each scaffold was assessed by gravimetry as $p = (1 - \rho_s/\rho_0)$, where ρ_s is the apparent density of the sample (mass-to-volume ratio) and ρ_0 is the density of the material (hydroxyapatite) of which the scaffold is fabricated.

The morphology of the sintered scaffolds was examined by scanning electron microscopy (SEM; JCM 6000 Plus Versatile Benchtop SEM, JEOL) at a voltage of 15 kV; the sample was sputter-coated with chromium (10 nm) prior to the analysis.

The compressive strength of scaffolds (σ_c) was determined by crushing tests as the L-to-A ratio, where *L* was the maximum load registered during the test and *A* was the initial cross-sectional area. Mechanical tests were performed by using an MTS System Corp. (Eden Prairie, MN, USA) apparatus (5-kN cell load, crosshead speed 1 mm/min). The elastic modulus (E) was determined from the linear region of the stress–strain curve.

Values of porosity, compressive strength and elastic modulus were expressed as average ± standard deviation calculated on 20 scaffolds.

2.2. Mechanical Modelling

The mechanical properties of scaffolds–σ_c and E–are expected to depend on both the constitutive properties of the solid materials (σ_0 and E_0) and the relative density $\varphi = \rho_s/\rho_0$. The total porosity can be expressed as $p = 1 - \varphi$. The relationships of σ_c and E to σ_0, E_0 and φ depends on the characteristics of pores and struts. Hence, models describing these relationships should be developed by considering the key architectural characteristics of scaffolds, which can be described as open-cell foams. A set of potentially suitable models (Table 1) was then selected from the literature based on their relevance in describing foam-like structures [15–21].

Table 1. Potentially suitable models to estimate σ_c and *E* of hydroxyapatite scaffolds.

Mechanical Property	Model Name	Model Equation	Reference
Compressive strength	Gibson–Ashby	$E = 0.2\sigma_0\varphi^{3/2}$	[15]
Elastic modulus	Gibson–Ashby	$E = E_0\varphi^2$	[16]
	Warren-Kraynik	$E = \dfrac{E_0\varphi^2\,(11 + 4\varphi)}{10 + 31\varphi + 4\varphi^2}$	[17]
	Zhu 1	$E = \dfrac{0.726\,E_0\varphi^2}{1 + 1.09\,\varphi}$	[17]
	Zhu 2	$E = \dfrac{1.009\,E_0\,\varphi^2}{1 + 1.514\,\varphi}$	[17]
	Gan	$E = \dfrac{E_0\,\varphi^2}{1 + 6\varphi}$	[19]
	Roberts–Garboczi	$E = E_0\left(\dfrac{\varphi - \varphi_0}{1 - \varphi_0}\right)^m,\ \varphi > 0.20$ $E = E_0 C\varphi^n,\ \varphi \leq 0.20$	[20]
	Nie	$E = E_0\,[3.32\,(1 - \varphi)^3 - 7.37\,(1 - \varphi)^2 + 4.98(1 - \varphi) - 0.92]$	[21]

The classical models used to estimate σ_c and *E* of foam-like porous solids are those developed by Gibson and Ashby [15], who established a direct correlation of both parameters with φ by means of two distinct power laws with similar form.

The E-φ relationship in open-cell porous solids has also been modelled using geometrical or numerical approaches. Warren and Kraynik [16] proposed a 3D foam model using a tetrahedral unit cell, while Zhu et al. [17] adopted a tetrakaidekahedral cell-based lattice in their modelling studies (Zhu 1 model). The latter research group also proposed a refinement of the model under the assumption, first introduced by Kraynik and Warren [18], that the edge cross-sections are plateau borders rather than equilateral triangles (Zhu 2 model) [17].

While the Gibson and Ashby, Warren and Kraynik, Zhu 1 and Zhu 2 models involve the analytical derivation of equations from physical and geometrical assumptions, other authors have proposed numerical approaches relying on finite element modelling (FEM) on a given geometry. Gan et al. [19] used random 3D Voronoi cells to model the whole volume of the open-cell foam, and fitted their FEM results with the model equations.

Roberts and Garboczi [20] reported highly accurate numerical simulations to predict the elastic modulus of a set of porous materials with various 3D architectures, including structures with open-cell intersections that mimic foam-like scaffolds. As shown in Table 1, they proposed two equations to estimate E according to the range of φ; the constants φ_0, m, n and C were numerically determined in [20] ($\varphi_0 = 0.029$, $m = 2.15$, $n = 3.15$ and $C = 4.2$).

Nie et al. [21] reported a similar approach using random 3D Laguerre–Voronoi computational models for open-cell foams and fitted the FEM results to obtain an E-φ equation.

The models collected in Table 1 were used to estimate σ_c and E of hydroxyapatite scaffolds produced by DLP-based vat photopolymerization. The results were compared with experimental data and analysed by Student's *t*-test (statistical significance set at $p < 0.05$).

3. Results and Discussion

Figure 1a,b show the morphology and microstructural details of the hydroxyapatite scaffolds produced in this work by vat photopolymerization. The scaffolds had a foam-like 3D architecture that replicated the starting template (polyurethane sponge) used in the printing system's CAD file. The traces of the layers created during the DLP printing process are visible in Figure 1c, which also reveals dense scaffold struts without internal channels that weaken the scaffold, as instead observed in other studies dealing with conventional foam-replica method [22]. A well-consolidated ceramic foam was obtained (Figure 1c), which was then expected to also have adequate mechanical properties.

The total porosity of the scaffolds (81 ± 2 vol.%) was comparable to that of human cancellous bone [12] and, therefore, suitable for osseous applications. A comprehensive analysis of pore-related architectural properties of these hydroxyapatite scaffolds was reported in a recent work [23].

An example of stress–strain curve is displayed in Figure 2 and shows the typical jagged profile of cellular ceramics as they fracture. Multiple peaks are associated with multiple fracture events that occur during the compression test [24]. After a first peak, a fluctuation of the load occurred (progressive fracture of the scaffold struts); when a second peak was reached, scaffold failure was then reached.

The scaffold compressive strength was 1.6 ± 0.8 MPa, fivefold higher than the strength assessed for hydroxyapatite scaffolds (around 0.3 MPa) produced in a previous study by foam-dipping/replica method and having analogous total porosity (82–86 vol.%) [25]. As discussed just above, this can be a direct consequence of well-densified struts (in the present scaffolds) with no residual channels inside, which weaken the structure and decrease the strength. Indeed, the DLP-based method is key to obtain such high-quality products.

Values of the mechanical properties of scaffolds are key to estimate and predict the implant behaviour in biomedical applications. The most commonly reported mechanical parameters, compressive strength and elastic modulus, may be difficult to determine experimentally for highly porous bioceramics, such as bone scaffolds. These properties mainly depend on total porosity which, on the contrary, is relatively easy to assess by gravimetry or image analysis. Therefore, the models reported in Table 1, relating compressive strength and elastic modulus to the total porosity $(1 - \varphi)$, can be used to predict the mechanical performance of scaffolds and optimize their design and fabrication process, avoiding the time-consuming and expensive trial-and-error approach.
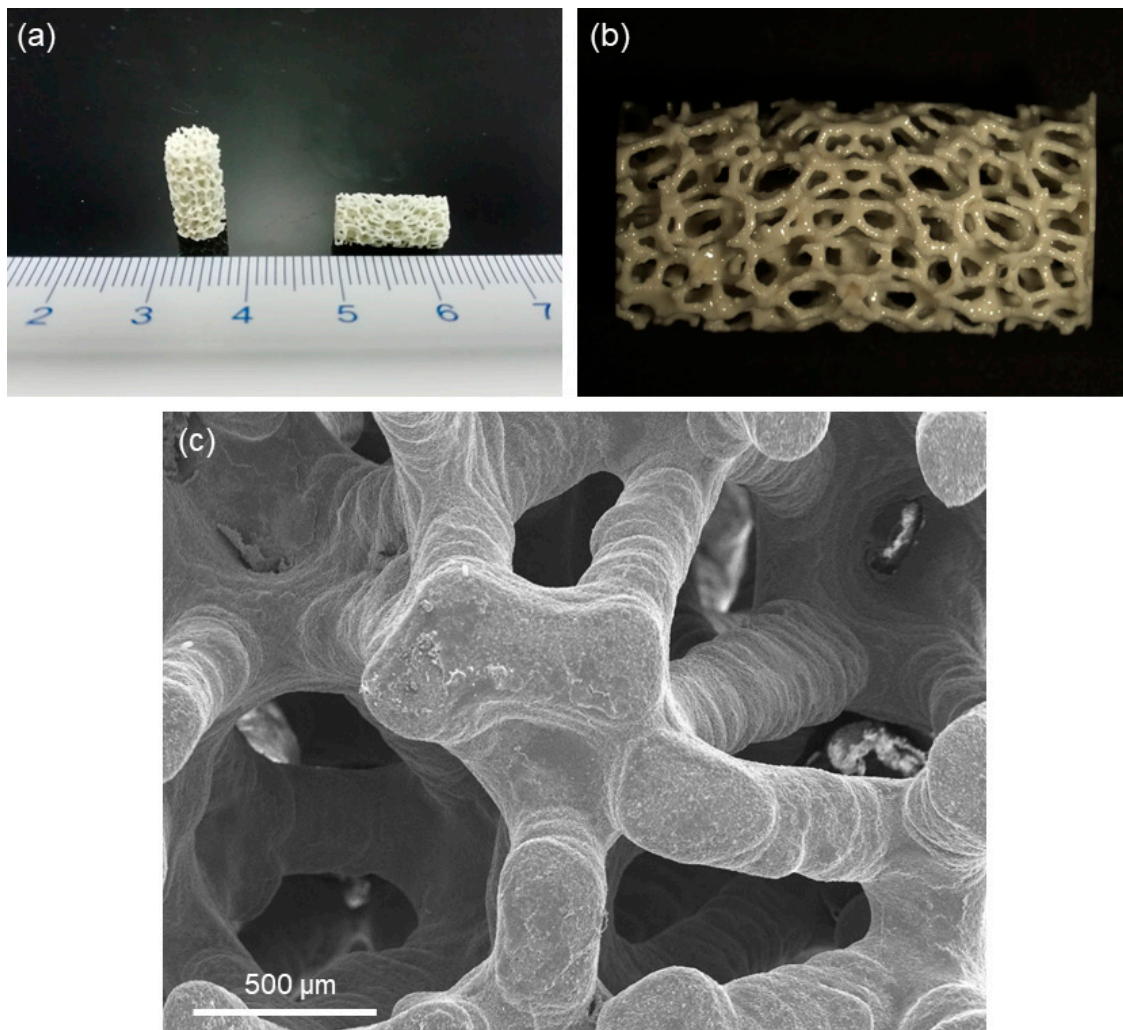
Figure 1. Results of the fabrication process: (**a**) cylindrical green bodies, (**b**) detail of the foam-like structure and (**c**) SEM micrograph of sintered hydroxyapatite scaffolds.
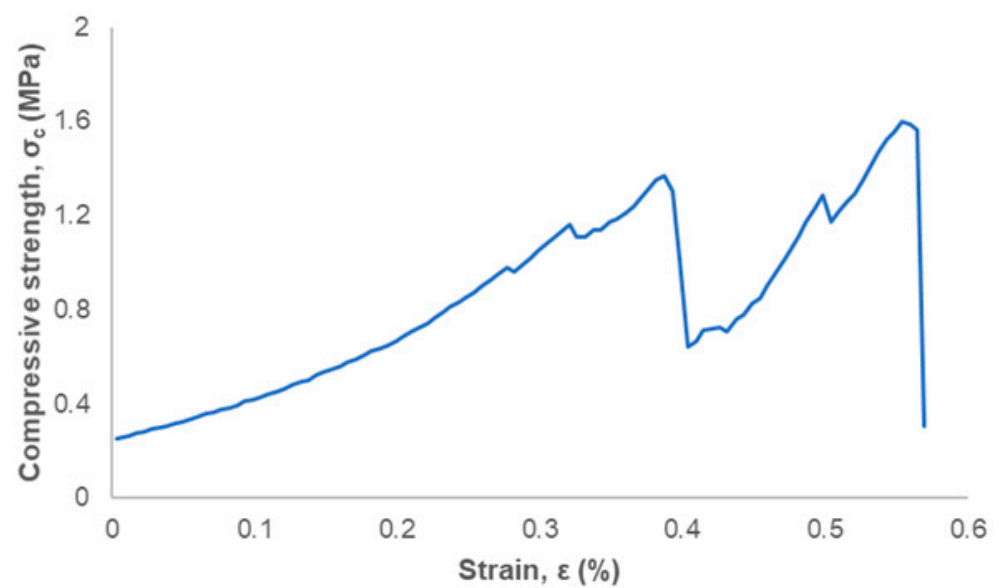

Figure 2. Typical stress–strain curve obtained after compressive test of hydroxyapatite scaffolds.

No statistically significant differences were found in compressive strength between the experimental values and the Gibson–Ashby model (Figure 3). This further extends the validity of the Gibson–Ashby equation, which has already been demonstrated to have high predictive capability for a variety of porous structures in several application fields. The exponent α in the φ^α term of the equation may also be different than $3/2$, depending on the specific material and microstructure considered; for example, $\alpha = 1.84$ was reported in the modelling of the compressive strength of 45S5 Bioglass®-derived glass-ceramic scaffolds produced by conventional foam replication (dipping method) [26]. In general, an α-range from 1.5 to 2.0 is comparable to that assessed for cancellous bone [27].
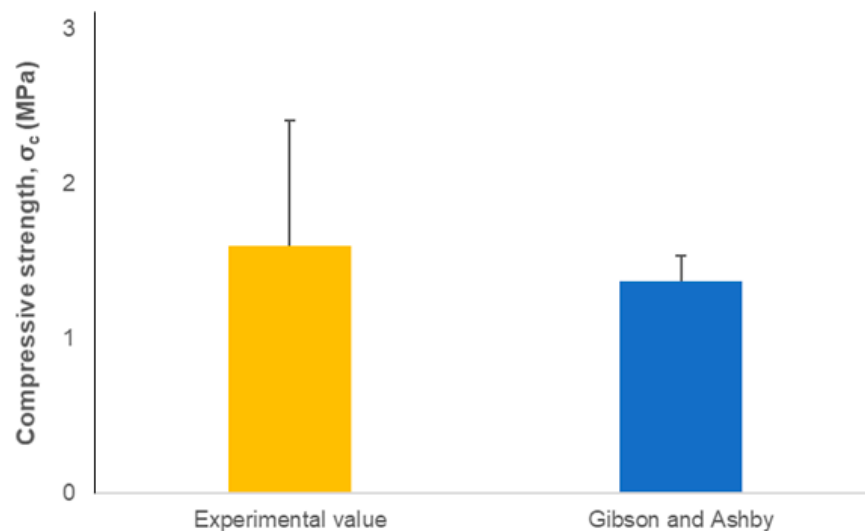

Figure 3. Compressive strength: comparison between the results from Gibson–Ashby model and experimental data ($n = 20$, $p < 0.05$).

In regard to the elastic modulus (Figure 4), the Gibson–Ashby, Warren and Kraynik, Zhu 2, and Roberts and Garboczi models had a good predictive capability, while the others (Zhu 1, Gan, and Nie models) provide statistically different estimates compared to the experimental results. The Gibson–Ashby model has already been applied to predict the elastic modulus of biomedical scaffolds. For example, Fu et al. [28] applied this density-power-law model to estimate the elastic modulus of foam-replicated 13–93 bioactive glass scaffolds with a total porosity of 85 vol.%. The Gibson–Ashby model was also predictive over a wide range of porosity (from 52 to 86 vol.%) in 45S5 Bioglass® foams [29]. As shown in Table 1, the Roberts and Garboczi model for high-porosity solids ($\varphi \leq 0.20$) has a similar density-power-law form as the Gibson and Ashby equation, although the constant and exponent are different; thus, it was not surprising that this model has a good predictive capability for foam-like structures as well.

The set of equations implemented in the present work can be considered as an "off-the-shelf" tool for scaffold manufacturers to obtain mechanical estimations using total porosity (or relative density) as the unique needed input, if the constitutive properties of the solid struts (σ_0, E_0) are known. Other more sophisticated approaches are also available to predict the mechanical properties of biomedical scaffolds; for example, continuum micromechanics and homogenization theories have been applied to model hydroxyapatite scaffolds with good predictive results [29]. Fully computational models [30] and "hybrid" approaches based on both experiments (e.g., nanoindentations) and FEM-based numerical simulations [31] were also proposed following a strategy similar to that reported by Gan et al. [19]. However, these models require the knowledge and quantification of the micro-architectural characteristics of the scaffolds. Furthermore, they do not provide an output equation that can be easily applied, such as the set reported in Table 1. In addition, the overall modelling procedure is complex and time-consuming, requiring expensive equipment (e.g., micro-computed tomography) and large computational facilities.
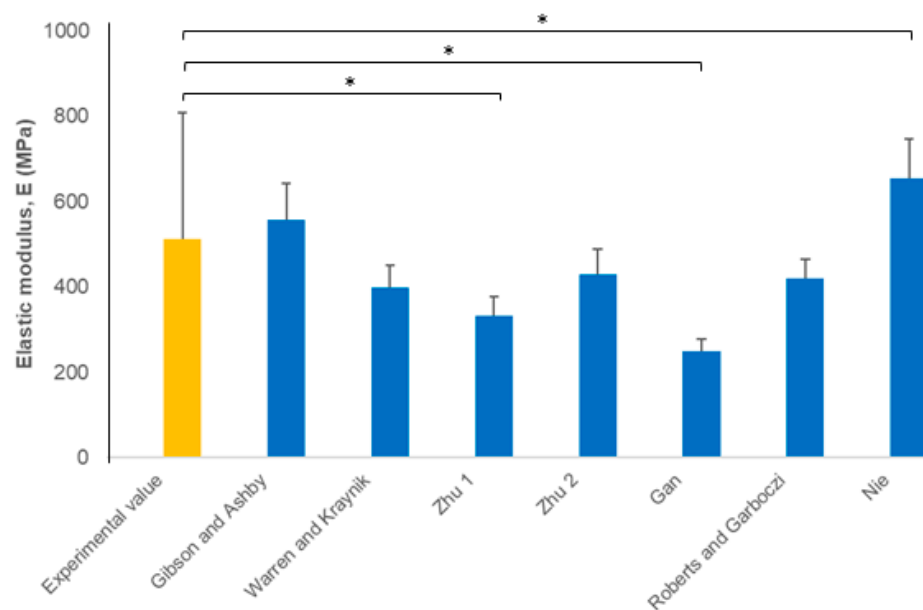
Figure 4. Elastic modulus: comparison between the results from the models listed in Table 1 and experimental data ($n = 20$, * $p < 0.05$).

4. Conclusions

A set of analytical or numerical models have been applied to determine the mechanical properties of hydroxyapatite scaffolds fabricated by DLP-based vat photopolymerization, with the aim to predict and compare it to experimental results. The classical density-power-law relation (Gibson and Ashby model) was suitable to predict the scaffold compressive strength based on total porosity. A similar equation (Gibson and Ashby second-order power law) worked well to describe the dependence of elastic modulus on porosity. In the latter case, other models were also found appropriate (Warren and Kraynik, Zhu 2, Roberts and Garboczi) for these type of high-porosity foam-like scaffolds. The other models may be suitable when applied to porous ceramics with other porosity ranges or different porous architecture (e.g., solids with closed pores).

References

1. Hulsart Billström, G.; Blom, A.W.; Larsson, S.; Beswick, A.D. Application of scaffolds for bone regeneration strategies: Current trends and future directions. *Injury* **2013**, *44*, S28–S33. [CrossRef]
2. Boskey, A.L. Mineralization of bones and teeth. *Elements* **2007**, *6*, 385–392. [CrossRef]
3. Gomes, D.S.; da Cunha Santos, A.M.; de Araújo Neves, G.; Menezes, R.R. A brief review on hydroxyapatite production and use in biomedicine. *Ceramica* **2019**, *65*, 282–302. [CrossRef]
4. Suchanek, W.; Yoshimura, M. Processing and properties of hydroxyapatite-based biomaterials for use as hard tissue replacement implants. *J. Mater. Res.* **1998**, *13*, 94–117. [CrossRef]
5. Dorozhkin, S.V. Bioceramics of calcium orthophosphates. *Biomaterials* **2010**, *31*, 1465–1485. [CrossRef]
6. Kumar, A.; Kargozar, S.; Baino, F.; Han, S.S. Additive manufacturing methods for producing hydroxyapatite and hydroxyapatite-based composite scaffolds: A review. *Front. Mater.* **2019**, *6*, 313. [CrossRef]

7. Potestio, I. Lithoz: How lithography-based ceramic AM is expanding the opportunities for technical ceramics. *Powder Inject. Mould.* **2019**, *13*, 2–5.

8. Feng, C.; Zang, K.; He, R.; Ding, G.; Xia, M. Additive manufacturing of hydroxyapatite bioceramic scaffolds: Dispersion, digital light processing, sintering, mechanical properties, and biocompatibility. *J. Adv. Ceram.* **2020**, *9*, 360–373. [CrossRef]

9. Fiume, E.; Ciavattini, S.; Verné, E.; Baino, F. Foam replica method in the manufacturing of bioactive glass scaffolds: Out-of-date technology or still underexploited potential? *Materials* **2021**, *14*, 2795. [CrossRef]

10. Baino, F.; Magnaterra, G.; Fiume, E.; Schiavi, A.; Tofan, L.P.; Schwentenwein, M.; Verné, E. Digital light processing stereolithography of hydroxyapatite scaffolds with bone-like architecture, permeability, and mechanical properties. *J. Am. Ceram. Soc.* **2022**, *105*, 1648–1657. [CrossRef]

11. Hing, K.A. Bioceramic bone graft substitutes: Influence of porosity and chemistry. *Int. J. Appl. Ceram. Technol.* **2005**, *2*, 184–199. [CrossRef]

12. Karageorgiu, V.; Kaplan, D. Porosity of 3D biomaterial scaffolds and osteogenesis. *Biomaterials* **2005**, *26*, 5474–5491. [CrossRef] [PubMed]

13. Ghayor, C.; Bhattacharya, I.; Guerrero, J.; Özcan, M.; Weber, F.E. 3D-Printed HA-Based Scaffolds for Bone Regeneration: Microporosity, Osteoconduction and Osteoclastic Resorption. *Materials* **2022**, *15*, 1433. [CrossRef] [PubMed]

14. Miguez-Pacheco, V.; Hench, L.L.; Boccaccini, A.R. Bioactive glasses beyond bone and teeth: Emerging applications in contact with soft tissues. *Acta Biomater.* **2015**, *13*, 1–15. [CrossRef]

15. Gibson, L.J.; Ashby, F. The mechanics of three-dimensional cellular materials. *Proc. R. Soc. Lond. A* **1982**, *382*, 43–59.

16. Warren, W.E.; Kraynik, A.M. The linear elastic properties of open-cell foams. *J. Appl. Mech.* **1988**, *55*, 341–346. [CrossRef]

17. Zhu, H.X.; Knott, J.F.; Mills, N.J. Analysis of the elastic properties of open-cell foams with tetrakaidecahedral cells. *Mech. Phys. Solids* **1997**, *45*, 319–343. [CrossRef]

18. Kraynik, A.M.; Warren, W.E. The elastic behavior of low-density cellular plastics. In *Low Density Cellular Plastics*; Hilvard, N.C., Cunningham, A., Eds.; Chapman and Hall: London, UK, 1994; pp. 187–225.

19. Gan, Y.X.; Chen, C.; Shen, Y.P. Three-dimensional modeling of the mechanical property of linearly elastic open cell foams. *Int. J. Solids Struct.* **2005**, *42*, 6628–6642. [CrossRef]

20. Roberts, A.P.; Garboczi, E.J. Computation of the linear elastic properties of random porous materials with a wide variety of microstructure. *Proc. R. Soc. Lond. A* **2002**, *458*, 1033–1054. [CrossRef]

21. Nie, Z.; Lin, Y.; Ton, Q. Computational modeling of the elastic property of three-dimensional open cell foams. *Arch. Metall. Mater.* **2018**, *63*, 1153–1165.

22. Chen, Q.Z.; Thompson, I.D.; Boccaccini, A.R. 45S5 Bioglass®-derived glass-ceramic scaffolds for bone tissue engineering. *Biomaterials* **2006**, *27*, 2414–2425. [CrossRef] [PubMed]

23. Schiavi, A.; Fiume, E.; Orlygsson, G.; Schwentenwein, M.; Verné, E.; Baino, F. High-reliability data processing and calculation of microstructural parameters in hydroxyapatite scaffolds produced by vat photopolymerization. *J. Eur. Ceram. Soc.* **2022**, *42*, 6206–6212. [CrossRef]

24. Gibson, L.J. Modelling the mechanical behavior of cellular materials. *Mater. Sci. Eng. A* **1989**, *110*, 1–36. [CrossRef]

25. Kim, H.W.; Knowles, J.C.; Kim, H.E. Hydroxyapatite porous scaffold engineered with biological polymer hybrid coating for antibiotic Vancomycin release. *J. Mater. Sci. Mater. Med.* **2005**, *16*, 189–195. [CrossRef] [PubMed]

26. Baino, F.; Fiume, E. Elastic mechanical properties of 45S5-based bioactive glass-ceramic scaffolds. *Materials* **2019**, *12*, 3244. [CrossRef]

27. Keller, T.S. Predicting the compressive mechanical behavior of bone. *J. Biomech.* **1994**, *27*, 1159–1168. [CrossRef]

28. Fu, Q.; Rahaman, M.N.; Bal, B.S.; Brown, R.F.; Day, D.E. Mechanical and in vitro performance of 13-93 bioactive glass scaffolds prepared by a polymer foam replication technique. *Acta Biomater.* **2008**, *4*, 1854–1864. [CrossRef]

29. Fritsch, A.; Dormieux, L.; Hellmich, C.; Sanahuja, J. Mechanical behavior of hydroxyapatite biomaterials: An experimentally validated micromechanical model for elasticity and strength. *J. Biomed. Mater. Res. A* **2009**, *88*, 149–161. [CrossRef]

30. Tagliabue, S.; Rossi, E.; Baino, F.; Vitale-Brovarone, C.; Gastaldi, D.; Vena, P. Micro-CT based finite element models for elastic properties of glass-ceramic scaffolds. *J. Mech. Behav. Biomed. Mater.* **2017**, *65*, 248–255. [CrossRef]

31. Farina, E.; Gastaldi, D.; Baino, F.; Verné, E.; Massera, J.; Orlygsson, G.; Vena, P. Micro computed tomography based finite element models for elastic and strength properties of 3D printed glass scaffolds. *Acta Mech. Sin.* **2021**, *37*, 292–306. [CrossRef]